A topographically controlled upwelling center off southern Vancouver Island

by Howard J. Freeland[1] and Kenneth L. Denman[1]

ABSTRACT

From January 1979 to June 1981 an oceanographic experiment off the west coast of Canada provided a unique view of a large annual upwelling event. The upwelling is driven by an interaction between the large scale coastal current systems and a narrow canyon that cuts the continental shelf. This interaction allows water to be raised from depths much greater than those normally expected from the classical wind-driven upwelling mechanisms. The water upwelled is dense, very low in dissolved oxygen and is rich in nutrients; it originates from the California Undercurrent.

A nonlinear theoretical model of the canyon/current interaction is developed including substantial stratification. The model succeeds in reproducing the salient observations.

1. Introduction

In January 1979 a large experiment was initiated to study the oceanographic characteristics of the Vancouver Island continental shelf. The intensive phase of this experiment ended in June 1981, though some work is continuing. The area is interesting for a number of reasons:

i) Despite the presence of several major oceanographic projects quite close by, such as CUEA, the west coast of Canada remained virtually unexplored.

ii) There are a number of maps available of "the circulation" of the Pacific Ocean, see for examples Tabata (1965), Hickey (1979) and Brekhovskikh (1980). These are all based on large volumes of hydrographic data and all paint the North Pacific with a very broad brush, but it is remarkable that they do agree on many major points. Notably, there is a steady current, the west wind drift, that crosses the bulk of the Pacific Ocean from west to east between latitudes 45N and 50N. At about the latitude of southern Vancouver Island the current splits into the southbound California Current and the northbound Alaska Current. It is quite unclear whether the oceanic regions adjacent to Vancouver Island belong to the Alaska Gyre system, the California Current system, or possibly neither.

1. Institute of Ocean Sciences, P.O. Box 6000, Sidney, B.C., Canada, V8L 4B2.

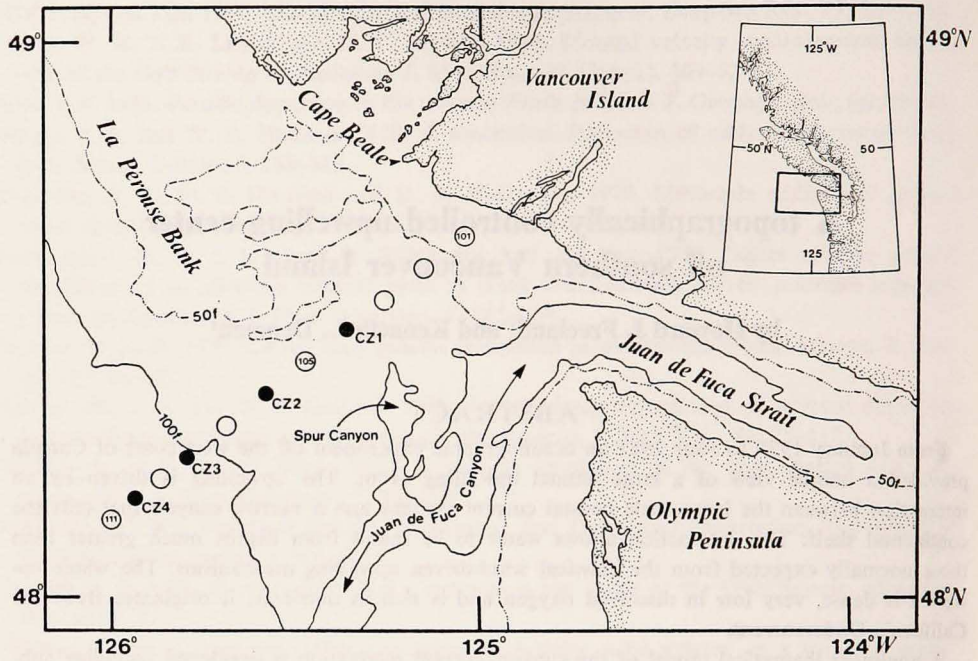

Figure 1. The study region off southern Vancouver Island. Circles mark the CTD locations constituting line 1, stations 101 to 111, the darkened circles are also mooring locations. To a good approximation the shelf edge is delineated by the 100 fathom (180 m) contour.

iii) The wind systems to the south of Vancouver Island are extremely favorable for upwelling, at least during the summer. The analyses of the climatic wind systems published by Bakun (1975) or by Nelson (1977) indicate that Vancouver Island is about at the northerly limit of the region where a substantial upwelling season is normally expected.

The region of intensive study, see Figure 1, is small; however, it has a rich and complex bathymetry that, as we will show, generated a rich and interesting oceanography. The region is bounded to the northeast by Vancouver Island and to the east by the coastline of Washington State. Between these two is the Strait of Juan de Fuca. Cutting the continental shelf into distinct northern and southern regions is a major submarine canyon, the Juan de Fuca Canyon. This canyon is narrow (about 7 km wide) and is deep throughout its length. It also has several sharp bends in its path and from one of these a second canyon heads northward, shallowing as it does so, until it disappears on the continental shelf. This canyon, a spur off the side of the Juan de Fuca Canyon, has no official name and, for convenience, we nicknamed it the "Spur Canyon." To the north of the Spur Canyon is a large fishing bank, La Pérouse Bank; there are also several other small banks in the study area, but La Pérouse Bank is the only one that is larger than the local internal Rossby radius of

deformation and so is the only one likely to be able to modify substantially the large scale geostrophic flows.

Besides being exposed to forcing from the Pacific Ocean and the local winds, the region of interest is also exposed to forcing from the Strait of Juan de Fuca. The Strait is a long narrow channel with a large freshwater source (the Fraser River) at its eastern end and so behaves like a large estuary. The outflowing water is fairly well mixed with ocean water, and so the salinity contrast between the upper (outflowing) and lower (inflowing) layers is quite small, typically 1 to 1½ ppt, however, the transport in the upper layer, typically $8 \times 10^4 m^3/s$, is large. The Strait is 20 km wide and that distance is almost exactly the local Rossby radius. Hence, it should come as no surprise that the boundary between the in- and out-flowing layers is sensibly tilted so that both flows are intensified to the right. According to Huggett *et al.* (1976) the boundary between the two layers is at a depth of about 140 m on the north coast and actually breaks the surface about 1 km from the southern coast. So we actually have a surface inflow along the southern (Washington) coast.

This paper concentrates on the physical oceanography of the southern Vancouver Island continental shelf. However, this effort was only part of a much larger investigation of the general oceanography of the whole Vancouver Island shelf and neighboring waters which was linked, in 1978, into a single effort run jointly by the various investigators. Denman *et al.* (1981) reported on preliminary results concerning the biology and physical oceanography off southern Vancouver Island. Crawford and Thomson (1982) and Thomson and Crawford (1982) described the tidal currents along the whole coast of Vancouver Island, discovering a diurnal shelf wave. Stucchi (1982) studied shelf/fjord exchanges in Alberni Inlet (top-center in Fig. 1); Mackas *et al.* (1980) and Mackas and Sefton (1982) studied phytoplankton and zooplankton community structures in relation to physical factors. Where necessary we will draw upon the results of these studies.

2. The observations

The data used in this paper consist of current meter mooring and hydrographic data. Four moorings indicated in Figure 1 as CZ4, CZ3, CZ2 and CZ1 were deployed in April 1979 and maintained until June of 1981. The moorings were all subsurface, the top buoyancy was at about 45 m depth and intermediate buoyancy, about half way down the mooring was also used. Current meters were deployed at depths of 50 m and 100 m on all moorings. In addition CZ3, on the shelf edge, carried a current meter at 200 m after June 1980, and CZ4, on the continental slope in water 800 m deep, carried current meters at depths of 250 m and 500 m. All current meters were Aanderaa RCM4's. A fifth mooring was deployed in a narrow canyon close to Cape Beale for a short time. The deep currents at this site are heavily guided by the canyon.

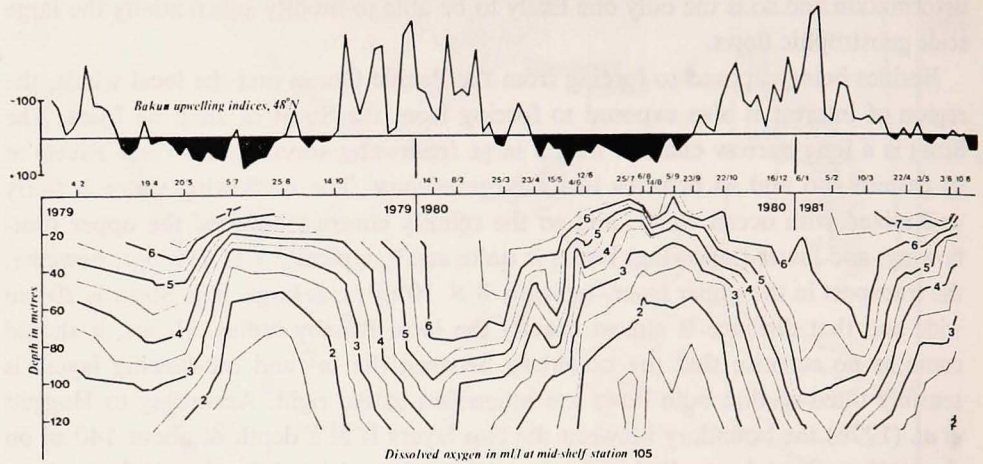

Figure 2. Time series of dissolved oxygen concentration, in ml/1, at the mid-shelf station 105, and the Bakun upwelling index computed at 48N 125W.

Frequent CTD surveys were carried out along the mooring line, seven during 1979 and about 1 per month from January 1980 to June 1981, plus several extensive surveys. The stations along the mooring line are numbered from 101 (nearshore) to 105 (mid-shelf) to 111 on the continental slope beyond mooring CZ4 (Fig. 1).

3. The annual cycle in oxygen and density

In the early summer of 1979 we were astonished to see a rapid decline in the dissolved oxygen concentration at station 105 (shown on Fig. 1). A time series plot of 2½ years of oxygen measurements at that one site is shown in Figure 2 and clearly demonstrates the rapid decline, below about 30 m, that increases in severity with depth. The spring decline in oxygen is much faster than can be accounted for by biological oxygen demand. In the fall of 1979 conditions returned to 'normal' and remained fairly steady through the winter. In spring of 1980 we embarked on a more aggressive sampling scheme and saw a slow decline in dissolved oxygen followed by a sudden drop during the first few days of June. The low oxygen event persisted until the fall and disappeared abruptly in November. Almost exactly the same pattern was being repeated in 1981, up to June 10th, when the experiment ended during a period of rapid decline in dissolved oxygen.

The dissolved oxygen values observed on the continental shelf can be very low: values below 1.5 ml/1 are common in this region during the summer, and during summer 1979 a value of 0.78 ml/1 was observed close to station 105 near the bottom. We would expect such a periodic low oxygen environment to affect the local benthos.

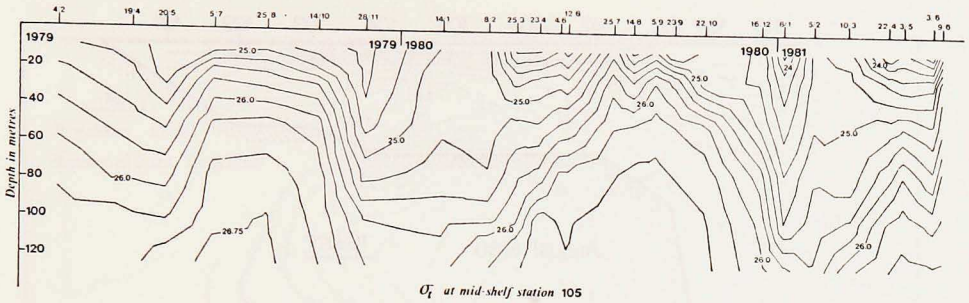

Figure 3. Time series of sigma-*t* at the mid-shelf station 105.

In Figure 3 we show a time series plot of sigma-*t* at station 105. It is evident that the same cyclic events are visible in the density field. In fact it is quite surprising just how tight a correlation between sigma-*t* and oxygen, below the surface layer, is maintained through the year. Clearly we are dealing with a feature that is physically, rather than biologically, controlled.

Returning to Figure 2, we have included a plot of the weekly averaged Bakun upwelling indices, computed at 48N 125W, where positive values are plotted downward, because a southward wind stress produces offshore surface flow and hence positive upwelling. It was evident in 1979, and more convincingly in 1980, that the temporal correlation between the local winds and the hydrographic series was weak. The low oxygen anomaly is phase shifted by about 90 days relative to the upwelling season, as defined by the Bakun upwelling indices. In 1981 a low oxygen event was developing as expected even though the area was experiencing weak upwelling-favorable winds relative to 1979 and 1980. After each summer it is possible that the low oxygen anomaly was swept off the shelf by the first major storm of the winter. As might be expected our data are comparatively poor from that part of the year.

Figure 4 depicts a cross-shelf section through the anomaly in August 1980 clearly showing a pool of low oxygen water on the continental shelf. This picture is typical of any section during the low oxygen anomaly period, though the anomaly usually extends a little closer to the edge of the continental shelf.

Figure 5 shows a contour map of sigma-*t* at a fixed depth in September 1980 demonstrating how local, in space, the phenomenon is. The anomaly of high sigma-*t* appears to be somewhat elongated alongshore, not a surprising result, and has a characteristic length and width of about 60 km and 40 km, respectively. The seaward side of the anomaly is bounded by a "front" or region of very large gradient which runs roughly along the edge of the continental shelf.

Only a few plots showing the structure of this anomaly are shown here, but during the part of the year that the anomaly is present we find the same pattern repeatedly. In particular the center of the anomaly does not appear to move by more than 5 km or so, probably less than the uncertainty of our ability to determine its position, and

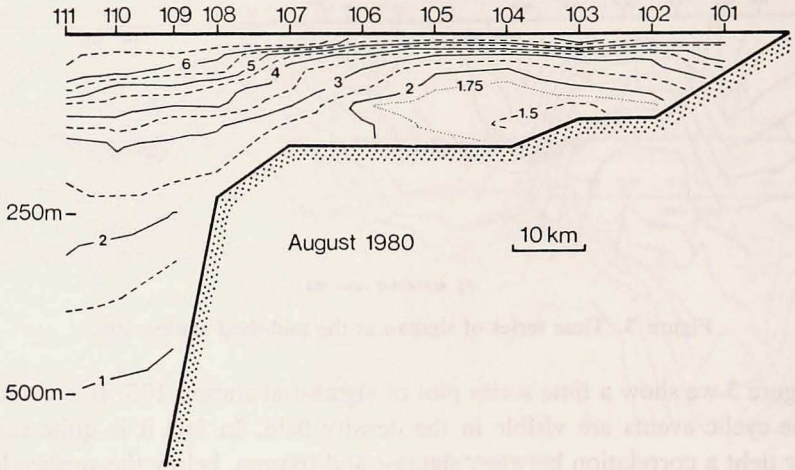

Figure 4. A typical section of dissolved oxygen concentration along line 1, in ml/1.

appears to remain closely associated with the northern terminus of the Spur Canyon. Almost any parameter we care to plot shows the same result, the eddy shows up clearly in temperature, salinity, sigma-*t*, nutrients, dissolved oxygen and velocities (to be discussed later), and the eddy appears to be a major source of nutrients for the southern Vancouver Island continental shelf, Denman *et al.* (1981) and Denman *et al.* (in preparation). The eddy even shows up in a parameter that is hard to quantify; in September 1980 one of us (H.J.F.) compiled a running contour map of temperature as quickly as data were acquired. As soon as the map was completed it was evident that the shape of the eddy could be seen almost as well in the distribution of large fishing vessels (fishing for hake) as seen on the ship's radar.

The contour maps of properties in the horizontal plane are all computed by the method of objective analysis as described by Bretherton *et al.* (1976). It is not appropriate to discuss the techniques in detail here; a paper on the statistical structure of oceanographic fields in the coastal environment, including physical, chemical and biological fields, is in preparation by Denman and Freeland (1983) which will discuss the parameters needed for objective mapping routines. It is well known that physical oceanographic fields in the coastal region are not isotropic; Kundu and Allen (1976), for example, discuss observations of shorter cross-shelf scales than along-shelf scales. For present purposes, however, it is of questionable value to attempt the objective mapping with anisotropic statistics, which involves only a trivial change to the mapping procedures. We have plotted a few examples and find no significant changes to the results quoted in this paper. If we wished to discuss the detailed shape of the eddy, then a detailed analysis of the anisotropy of the covariance field would be required. It is useful to note that in this paper all of the horizontal contour maps are computed using a single objective algorithm using a

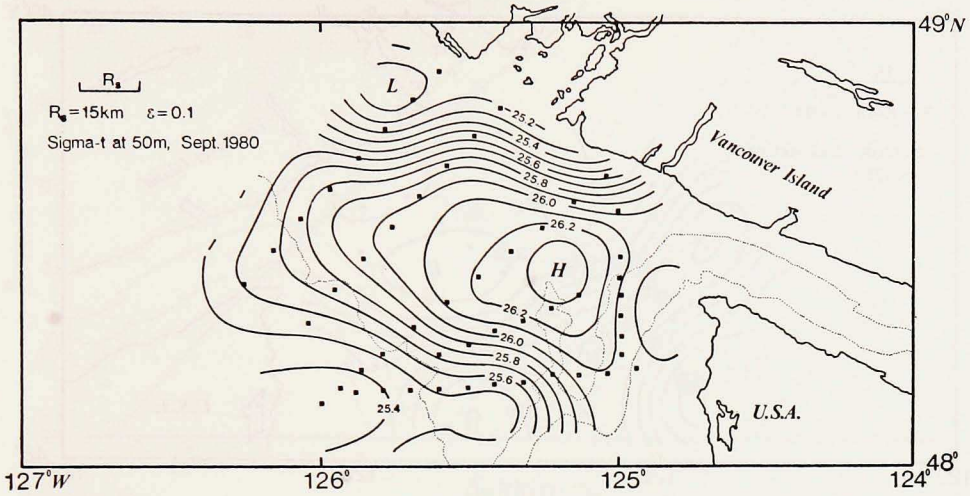

Figure 5. Contour map of sigma-t at 50 m during September 1980, a period when the eddy at the mouth of the Strait of Juan de Fuca was present. This map, and subsequent contour maps, were computed by the method of objective analysis, or optimal estimation, see text. On all maps R_s denotes a length scale and ϵ a noise level in the correlation function used. The 100 f. = 180 m depth contour is marked on the maps with a dotted line, this contour is useful to delineate the shelf edge and the positions of the canyons.

single specified set of statistics, hence, the set of maps form an internally consistent set. On each objective map to be presented the value of a parameter R_s is entered in the upper left. This is the distance to the first zero-crossing of the transverse velocity correlation function. In all maps a mean square noise level of 10% is assumed, this was estimated from 13 hour time series CTD observations.

Figure 6 shows a plot of a parameter τ, defined by Veronis (1972), on the surface sigma-t = 26.2 which varies in depth from 37 m at the center of the eddy to 110 m at the inshore or offshore edges. τ is a function of temperature and salinity that is orthogonal to sigma-t curves on a T/S plot. Though the actual values are of no consequence it is a convenient measure of how different two water masses are that share the same sigma-t value. It is not affected by seasonal changes that might make density more or less strongly determined by salinity or temperature. If two water masses have the same τ on any given sigma-t surface, then those two water masses are identical. On Figure 6 we see two regions of low τ, one in the middle of the continental shelf and one on the slope, these two regions are separated by a ridge of high τ running along the shelf edge. If these identical water masses have a common origin then water will have to travel from the continental slope to the middle of the shelf (or vice versa) effectively without passing through the space between. As we will see later that is almost what happens.

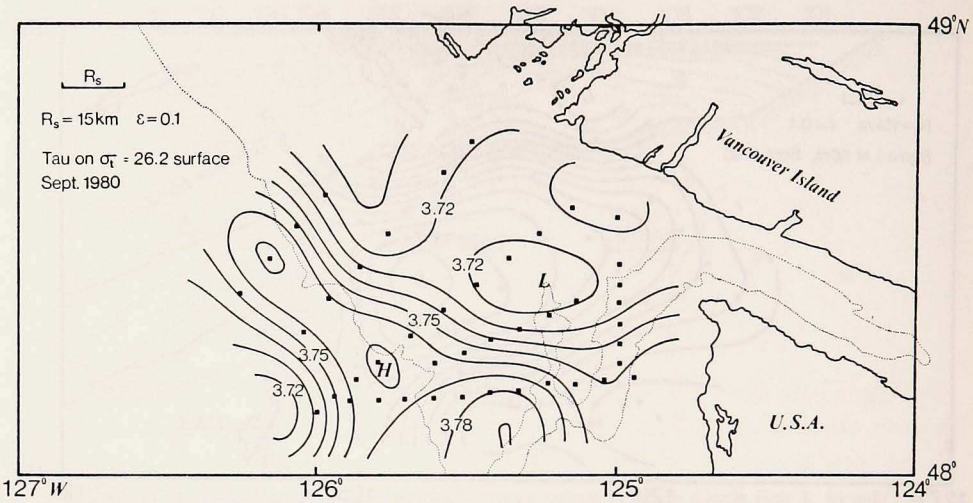

Figure 6. Tau on the surface sigma-t = 26.2, September 1980. For additional information see caption for Figure 5.

Finally we would like to discuss the possible origins of this low oxygen water. Figure 7 shows a T/S plot with data entered to show the annual cycle of the T/S relation at station 105. Also indicated are several historical observations of the T/S characteristics of the California Undercurrent at various locations. The entries are for the core of the undercurrent off S. California, N. California and a group off Oregon and Washington. The T/S relation at station 105, at 100 m, passes right through, and spends most of the summer, within this group of observations. If we represent all North Pacific water masses as mixtures of Equatorial and Sub-Arctic water masses then we can enter lines, shown in Figure 7, of constant fraction of equatorial water. Evidently the data indicate an increase during the summer months in the fraction of equatorial water on the shelf. This is surprising at first sight since, as will be shown in the next section, the dominant currents in the upper 100 m are from the north in summer and from the south in winter. Somehow, California Undercurrent water is being raised from depth and deposited on the continental shelf. The observations that this water is low in oxygen and high in nutrients further confirm the notion that the water has been away from the surface layer for a considerable time. However, to date there have been no direct observations of the California Undercurrent this far north. It is easy enough to say that water is raised from depth onto the continental shelf, however, substantial problems arise when one looks in detail at the implications.

i) Upwelling is normally considered to be a local response to local winds. Casual inspection of Figure 2 indicates that this is not so in this case.

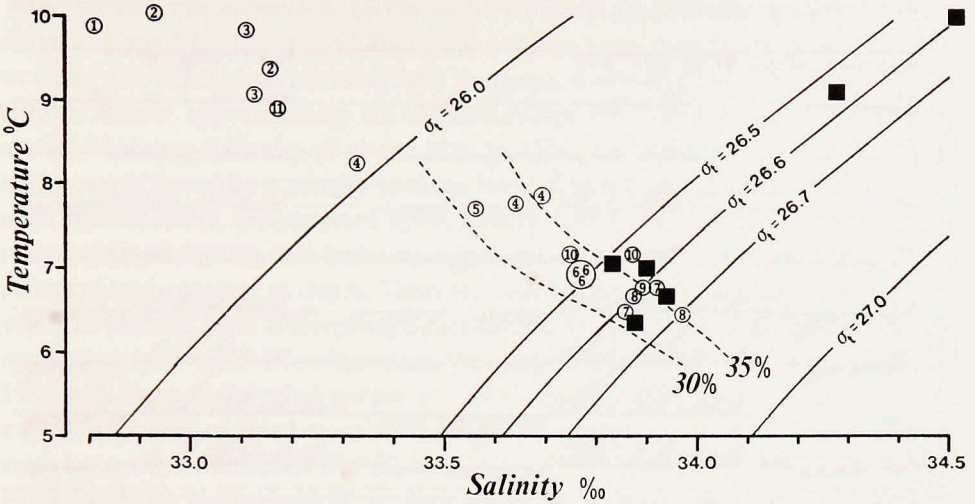

Figure 7. Temperature-Salinity correlation at station 105 at 100 m depth as a function of time. Circles with numbers indicate the observed T/S values for the specified month number. When more than one entry for a given month occurs in the diagram then those entries are for different years. Data are entered for the years 1979, 1980 and 1981. The rectangles show the T/S characteristics of the California Undercurrent, observations at the velocity core, from southern California, northern California and a group of four observations from Oregon and Washington.

ii) Upwelling of the classical kind can raise water from only moderate depths below the shelf break, a depth of 250 m might be permitted for the densest water. To satisfy T/S and oxygen observations we need to raise the densest water from 450 m.

iii) Upwelling is normally expected to have the same frequency content as the wind forcing; i.e., we should have upwelling events of, say, 10 days or so in duration. Instead we see one event per year that lasts for longer than 100 days.

iv) There should be nothing particularly special about the response at this location. We see about the same forcing due to the wind off northern Vancouver Island but in fact the annual cycles that do occur are of a much smaller magnitude than the events shown in Figure 2.

The conclusion must be that we are not dealing with an upwelling event of the classical kind, but rather a special locally determined phenomenon.

4. The velocity field

In Figure 8 we show vector plots of currents from the four moorings CZ4, CZ3, CZ2 and CZ1 and the Bakun upwelling index. The raw data from the current meters

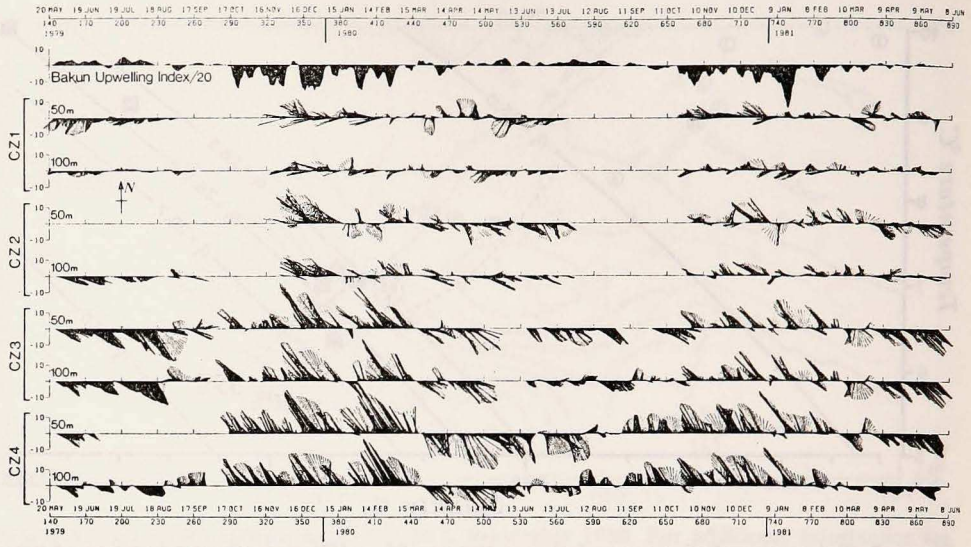

Figure 8. Vector plots of currents at 50 m and 100 m at the four principal mooring sites, and the Bakun Upwelling Index at 48N 125W, from 20 May 1979 to 8 June 1981.

were initially filtered with a Lanczos-cosine filter, half-power point at 40 hours, and subsampled at 12 hour intervals. That procedure alone should effectively eliminate ageostrophic fluctuations, to be tested later, however, for Figure 8 the data, including the upwelling indices, were filtered additionally with a 6 day running mean filter. Gaps in the data (when a mooring was being serviced) of less than 3 days were filled by linear interpolation prior to application of the running mean filter.

On the continental slope (CZ4) and at the shelf edge (CZ3) we see a clear annual cycle emerging in the current field. Currents are strongly polarized parallel to the local bathymetry with northward flow of, typically, 20 cm/s in the winter and southward flow in the summer. An abrupt transition in currents occurred on 18th March, 1980 at CZ3 and 4 days later at CZ4. This transition marks a distinct separation in time between the winter and summer regimes and has been called, by Huyer *et al.* (1979), the spring transition. We note that although the 1980 transition appears to be centered on 22nd March at CZ4 and 18th March at CZ3, the major change in the wind system occurred on about 8th of March, considerably earlier. This time separation was reversed in 1981 with the change from winter to summer conditions on about 28th March in the wind field and in the current field around the 6th of March at both moorings CZ3 and CZ4. The conclusion is, therefore, that the major seasonal cycles in currents are not strongly coupled to the local wind system. Strictly, some correlation must exist, of course, since both are dominated by annual cycles and are not in quadrature; what we doubt is the existence of a direct causal relationship.

In summer the magnitude of the wind stress is considerably greater between, roughly, Cape Mendocino and Point Conception even though the wind direction on either side of this band is essentially the same, southward alongshore, see Nelson (1977). Rather approximately we might consider the summer wind system to be confined between latitudes of about 32N to 42N. An analysis of a coastal current environment forced by a zonally-uniform band of steady equatorward winds limited in latitudinal extent was reported by McCreary (1981). He found a response in the region of direct forcing that included equatorward currents near surface and a deep poleward undercurrent at depth. However, this response propagated northward beyond the latitude band undergoing direct forcing at the speed of an internal Kelvin wave, about 1.5 m/s. If we compare the current transitions at CZ3 in 1980 and 1981 with those in the wind system at 39N (just south of Cape Mendocino) we find a regular pattern of wind transitions preceding current transitions. The winds reverse before the transitions at CZ3 by 4, 9, 3 and 5 days for the fall 1979, spring 1980, fall 1980 and spring 1981 events, respectively (Bakun, pers. comm.). Though the delay seems somewhat variable the relationship is more plausible than the attempt to fit the currents to the local wind systems. The average delay of 6 days suggests a northward propagating disturbance travelling at about 180 km/day, or 2.0 m/s, which is close to the speed expected for a first mode internal shelf wave.

Referring back to Figure 8 we see that annual cycles are not immediately apparent at moorings CZ1 and CZ2, both on the continental shelf. This is an illusion, in fact, that results from the absence of data at both of these sites for considerable parts of the summer; i.e., repeatedly one season. In 1979 moorings were lost to an intensive hake fishery that developed in mid-summer. In 1980 we had sufficient warning of a large increase in the fishing effort that we considered it wise to leave the sites unoccupied from mid-July onward to the next opportunity to redeploy the moorings. Careful examination shows a distinct seasonal cycle at CZ2 with flow predominantly to the NW in winter and to the SE in summer. An annual cycle still exists at CZ1 but is considerably weaker than at any of the other sites. We suspect that this might arise partially from the coastal current produced by the Juan de Fuca outflow.

At all sites the shear between 50 and 100 m is of interest. At the two offshore sites we see a high degree of visual correlation year round between the velocities at 50 and 100 m. Rather less obviously, but still visible, is a seasonal difference, 50 m and 100 m currents correlate better in the winter than in the summer. In the summer increased stratification allows larger geostrophic shears to develop so allowing greater differences. As we move inshore the seasonal difference steadily increases, until at CZ1 we have a high degree of visual similarity in the winter and early spring, but the 100 m currents at CZ1 appear simply to die away as the summer proceeds, both in 1979 and 1980. This type of seasonal variation in the intensity of low frequency fluctuations has been observed by Huyer *et al.* (1978) off the coast

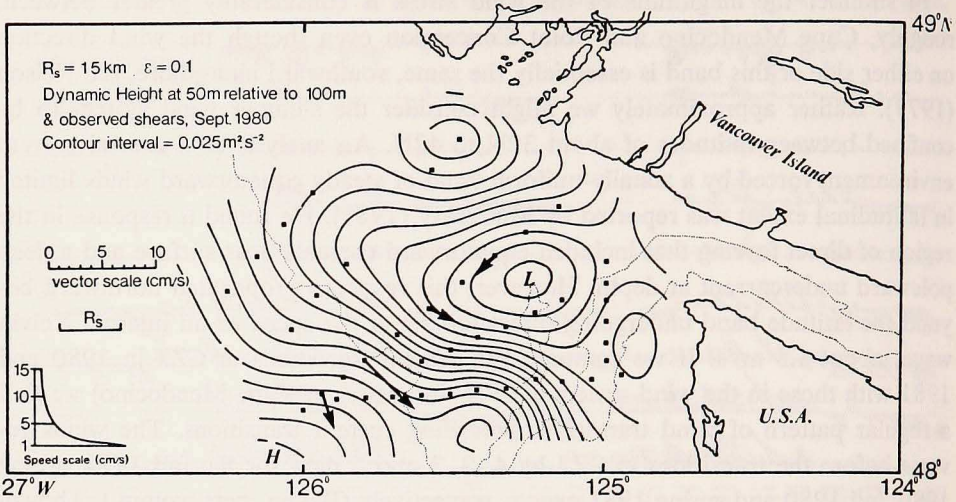

Figure 9. Dynamic height field at 50 m relative to 100 m and the observed shear vectors between 50 m and 100 m. Two speed scales are shown, one for the vectors (the linear scale) and one for computing the speeds from contour separations (the nonlinear scale). For further information see caption for Figure 5.

of Oregon. Here the variation is marked, and by June speeds are virtually nil at CZ1 at 100 m and all similarity with upper level flows disappears. This observation is consistent with the view developed in the previous section of a mound of (almost) stagnant water sitting on the continental shelf during the summer months. It appears that, as the upwelled water mounts up on the continental shelf, shear steadily increases and the deep velocities steadily decrease.

As these changes take place the flows remain in geostrophic balance. Figure 9 shows the dynamic height field computed for a period near the end of summer 1980. The dynamic heights are computed at 50 m relative to 100 m and the gradient of that field yields the shear between 50 m and 100 m standard current meter depths. The arrows entered on the contour map are the observed shear for that date from the moored current meters. Clearly the similarity of the vectors and contours confirms the view that the shelf flows are predominantly geostrophic. The vector from mooring location CZ4 does not fit the contours as well as the others, but it is right at the edge of the contoured field where one might expect errors to become large. Also sampling errors might be expected to be larger on the continental slope where resonant generation of internal tides might occur. Note that the objective analysis yields an estimate of the expected error; in all of these maps the contours were drawn only when the expected error was less than 0.7 standard deviations. The CZ4 shear vector is close to the edge of the error window within which contours are

permitted. Other maps of dynamic height have been computed and compared with the shear vectors and the agreement is as good as in this map in all cases.

A comment about the computation of the dynamic height maps and shear vectors is appropriate here. The maps are objectively computed, and as described earlier we are permitted to specify a noise level and the computer fits a surface through the observations to within this noise level, in all of these maps estimated to be 10% of the total variance. Hence, some information, presumably noise due to asynoptic sampling and local events such as internal waves, is discarded. We decided to match this process in the computation of the shear vectors. The complete records from the 50 m and 100 m current meters at the four moorings CZ1, 2, 3 and 4 were taken and separated into the 16 empirical orthogonal functions (4 moorings $\times$ 2 meters per mooring $\times$ 2 independent coordinates per meter = 16 records). The first two E.O.F.'s accounted for 92% of the total variance; i.e., close to the 90% accounted for in the dynamic height maps. In particular both of the first two E.O.F.'s appear to be significant and the eigenvectors are not dominated by any one site; the 3rd and higher modes all individually contribute little to the total variance and tend to be dominated by the signal at a single site. Hence, we feel well justified in representing the "observed shear" as that represented by the sum of the first two modes. The vectors on Figure 9 were computed in this way. Other maps and comparison with vectors will be presented in a later paper by Denman and Freeland.

On Figures 5, 6 and 9 a light dotted line has been used to mark the path of the 100 fathom (180 m) isobath. This isobath effectively delineates the shelf edge and clearly outlines the positions and shapes of the canyons. It can be seen on Figures 5, 6 and 9 (and other maps) that the eddy is always closely associated with the northern terminus of the Spur Canyon. The linkage of oceanographic properties to this canyon is striking and has led us to examine the possibility that some interaction between geostrophic currents and the canyon system was producing the large upwelling seen on the shelf. We have developed a model of canyon flows that accounts for the observed upwelling and which is described later. Essentially we hypothesize the following sequence of events:

i) In winter shelf edge currents are northbound and the Juan de Fuca outflow current is also northbound, along the coast.

ii) In early spring (say mid-March) the shelf edge current reverses (the spring transition) and a cyclonic eddy is spun up on the wide continental shelf. Stratification is initially weak so vertical shear is initially small.

iii) The eddy is quasi-geostrophic and flows over the Spur Canyon; however, the canyon width is about half the internal Rossby radius of deformation, so the geostrophic circulation in the eddy cannot be significantly influenced by the presence of the eddy.

iv) Since in early spring vertical shear is small, water parcels moving in the eddy experience an inward pressure gradient that is (largely) balanced by an outward Coriolis force. Near the bottom these forces are still felt; however, inside the Spur Canyon water parcels experience only the pressure gradient force since transverse motions are suppressed.

v) The inward pressure gradient forces a weak flow up the canyon to develop which advects water from the mouth of the canyon system onto the continental shelf.

vi) Water originally in the canyon system at the time of the spring transition flows onto the continental shelf, and accounts for the slow decline in dissolved oxygen levels seen between the spring transition and the rapid decline in oxygen levels.

vii) As water originating from the California Undercurrent passing the mouth of the Juan de Fuca arrives on the shelf, we observe the rapid decline in oxygen values seen in early June of each year.

viii) As dense water accumulates on the shelf horizontal density gradients increase, vertical shear increases (through the thermal wind relation) and the deep inward pressure gradient decreases. If water tends to flow back down the canyon the vertical shear will decrease which will tend to restore the inward pressure gradient.

5. Estimate of wind-driven upwelling

Before we proceed with our model of canyon ducted upwelling two points in our hypothesized sequence of events need to be clarified. First, we must demonstrate that the California Undercurrent does actually reach the latitude of Vancouver Island, and second, we must show that the classical model of wind-driven upwelling across the shelf-break cannot supply the anomalous water we observe on the shelf during the summer months.

In an attempt to observe the character of near-bottom currents we deployed a current meter about 10 m off the bottom at CZ3 (see Fig. 1) just seaward of the shelf-break. Figure 10 shows a plot of current vectors at all three depths on CZ3 from June 1980 to February 1981, and the Bakun upwelling index. Clearly visible is a sharp transition in the wind conditions on October 20th, 1980. During the summer we have a strong flow near surface and a somewhat weaker flow at 100 m, both to the south. A sharp transition in the 50 m and 100 m currents occurs on November 1st, 1980, 10 days after the transition in the wind system. However, the flow as seen at 200 m is northward for all but a small fraction of the total time series. During the summer of 1980 then, we see clear evidence of a poleward under-

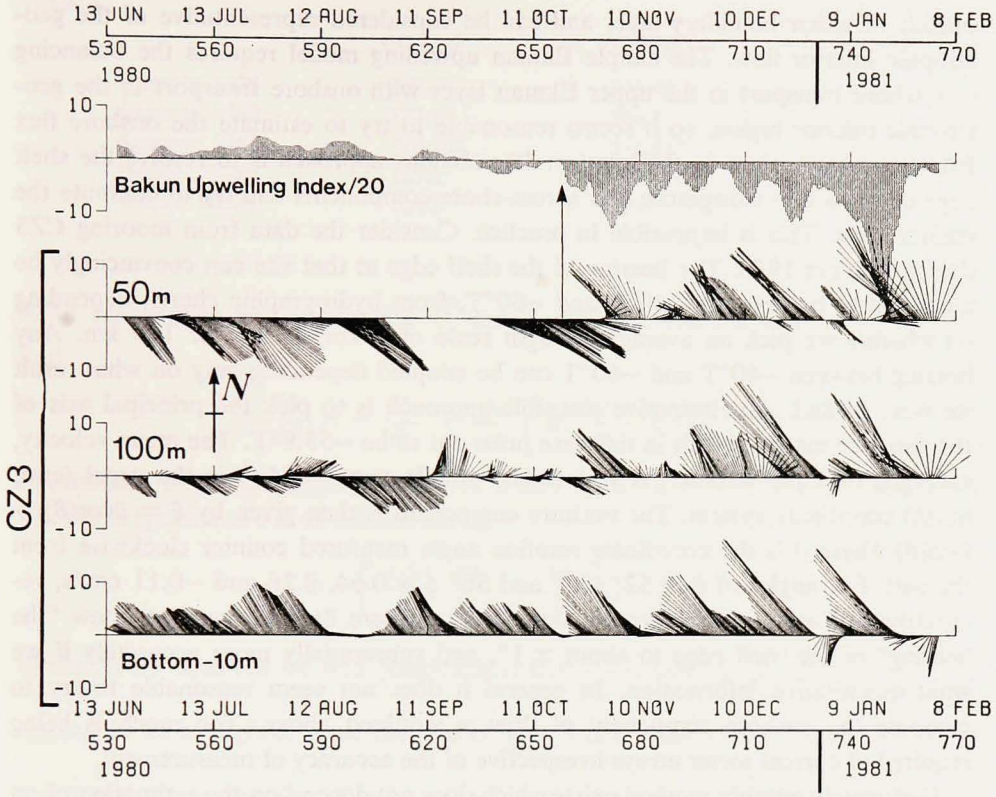

Figure 10. Vector plots of currents at 50 m, 100 m and 200 m at site CZ3 at the shelf edge to show the presence of a poleward undercurrent during the summer.

current at this mooring a couple of kilometers seaward of the shelf break in 210 meters of water.

During much of the summer, as shown in Figure 2, the southern Vancouver Island shelf is subjected to an upwelling season. The question naturally arises, do we actually observe upwelling over the shelf break and is there any way that it could account for the dense water on the continental shelf? We have claimed that wind-driven upwelling could not supply the observed upwelling; we should attempt to demonstrate that unequivocally.

From simple theory we expect the thickness of the upper Ekman layer to be $\delta = \sqrt{2A_v/f}$, Pedlosky (1979), and using $A_v = 55$ cm^2/sec, a value typical of Oregon strong upwelling systems reported by Halpern (1976), we find $\delta \sim 10$ m. The bottom boundary layer has a thickness $\delta_o \sim 0.3\ u_*/f$ where the friction speed u_* is about $0.03v_g$ and v_g is the geostrophic speed outside the boundary layer (see Weatherly and Martin, 1978). Taking a large value for $v_g \sim 25$ cm/sec, we find $\delta_o \sim 20$ m. Hence, our principal current meter depths of 50 m and 100 m are well

outside of either boundary layer and can be considered representative of the geostrophic interior flow. The simple Ekman upwelling model requires the balancing of offshore transport in the upper Ekman layer with onshore transport in the geostrophic interior region, so it seems reasonable to try to estimate the onshore flux from our observations in the interior. The obvious approach is to resolve the shelf edge currents into alongshore and across-shore components and try to compute the onshore flux. This is impossible in practice. Consider the data from mooring CZ3 during summer 1980. The bearing of the shelf edge at that site can convincingly be measured to be between −40°T and −60°T, from hydrographic charts, depending on whether we pick an averaging length scale of 1 km, 10 km or 100 km. Any bearing between −40°T and −60°T can be adopted depending only on what result we want to find. An alternative plausible approach is to pick the principal axis of the variance matrix, which in this case turns out to be −53.9°T. The mean velocity, averaged over the summer, is $\mathbf{v} = (8.80, -6.07)$ cm/s $= (\bar{u},\bar{v})$ in the usual (east, north) coordinate system. The onshore component is then given by $\xi = \bar{u}\cos(\theta) + \bar{v}\sin(\theta)$ where θ is the coordinate rotation angle measured counter clockwise from the east. For angles of $\theta = 52°$, 54° and 56° ξ is 0.64, 0.26 and −0.11 cm/s, respectively. Clearly, to observe the sign of the onshore flow we need to know "the bearing" of the shelf edge to about ± 1°, and substantially more accurately if we want quantitative information. In general it does not seem reasonable to try to compute the onshore component of flow as outlined above. Too much is being required of current meter arrays irrespective of the accuracy of measurement.

Fortunately another method exists which does not depend on the estimation of an uncertain bearing. Bryden (1978) described a method for estimating the vertical component of velocity from a single mooring. In summary we require hydrostatic, geostrophic flow, thus:

$$\left(\frac{\partial p}{\partial x}\ ,\ \frac{\partial p}{\partial y}\right) = \rho_o f(v, -u)$$

and

$$\frac{\partial p}{\partial z} = -\rho g$$

with z positive upward.
We derive the thermal wind relations

$$g\left(\frac{\partial}{\partial x}\ ,\ \frac{\partial}{\partial y}\right)\rho = \rho_o f \frac{\partial}{\partial z}(-v, u)\ .$$

In the absence of diffusion we can write the density conservation equation as:

$$\frac{\partial \rho}{\partial t} + u\frac{\partial \rho}{\partial x} + v\frac{\partial \rho}{\partial y} + w\frac{\partial \rho}{\partial z} = 0\ .$$

Table 1.

	θ (50 m)	θ (100 m)	w (m/day)
Summer 1979	300.5°	301.4°	0.43
Summer 1980	322.8°	324.1°	0.47
Summer 1981	318.78°	318.81°	0.01
Winter 79–80	129.0°	127.3°	−1.06
Winter 80–81	126.3°	123.2°	−1.23

After rearranging and eliminating $\frac{\partial \rho}{\partial x}$ and $\frac{\partial \rho}{\partial y}$ with the thermal wind equations we find:

$$w \frac{\partial \rho}{\partial z} = -\frac{\partial \rho}{\partial t} + \frac{\rho_o f}{g}\left[u \frac{\partial v}{\partial z} - v \frac{\partial u}{\partial z} \right].$$

Substituting polar coordinate versions of u and v; i.e., $u = s \cos \theta$ and $v = s \sin \theta$ where s is speed and θ is as defined earlier

$$w = \left[\frac{\rho_o f s^2}{g} \frac{\partial \theta}{\partial z} - \frac{\partial \rho}{\partial t} \right] \Big/ \frac{\partial \rho}{\partial z}.$$

In the above equation we find (empirically) that $\frac{\partial \rho}{\partial t}$ is usually extremely small and appears to be negligible. Since the sign of $\frac{\partial \rho}{\partial z}$ is fixed, negative, as long as stratification is stable then the sign of w is determined by the sign of $\frac{\partial \theta}{\partial z}$. For upwelling $\frac{\partial \theta}{\partial z} < 0$ or, θ increases downward. Table 1 lists values of the bearing at 50 m and 100 m, at the shelf break mooring, broken down into significant time intervals. Also listed are the computed values of vertical velocity.

It is encouraging that we find systematically positive values of w for the summer seasons and negative for the winter. Note, however, that for the purposes of this table "winter" and "summer" are defined with careful reference to the Bakun upwelling indices for each year. The vertical velocity appeared to be slightly larger in 1980 than in 1979 and indeed the Bakun Upwelling Index, averaged over the summer, was larger in 1980, 33.6 m³/s/100 m compared with 23.3 in 1979. The observed value of w listed for summer 1981 is small, and indeed the upwelling indices were particularly weak up to June 1981, when the experiment ended, the mean upwelling index was only 1.3 m³/s/100 m. Using some rather bold assumptions we can convert the observed values of vertical velocity to upwelling indices. We assume that the observed w is a value "typical" of the whole water column below the surface Ekman layer and divide w by the bottom slope to get the onshore component of velocity. Evidently this procedure neglects any baroclinic effects that might tend to give the onshore component of flow some vertical structure and so should be re-

garded only as a scaling argument to get the approximate size of the onshore component of flow. However, despite the lack of vertical structure, this approach at least yields an unambiguous observation of the sign of the onshore component of flow which is something the methods outlined earlier were not capable of yielding. Thus a vertical velocity of 0.5 m/day at this site is equivalent to a Bakun Upwelling Index of 7 $m^3/s/100$ m, or an interior onshore flow of 0.037 cm/s, and so we observe that the vertical velocities measured are smaller, by a factor of four, than those expected from the magnitude of the forcing. A typical summer value of the Bakun Upwelling Index for this area, 25 $m^3/s/100$ m, could supply the volume of water having oxygen concentration less than 2 ml/l, in Figure 4, in about 130 days. The observed value of around 6 $m^3/s/100$ m would supply that water in about 470 days. The former figure is too long and the latter is much too long. Hence, though we verify that upwelling of the classical kind does occur off the west coast of Vancouver Island we must reject it as the mechanism for supplying the dense low oxygen water that is observed to accumulate each year. This is a robust conclusion even with the neglect of baroclinic effects. Inclusion of baroclinicity might tend to increase the observed onshore flow substantially above the 6 $m^3/s/100$ m, but it is necessary to increase that flow by at least an order of magnitude before we can claim that the wind is capable of supplying the upwelled water.

6. Flow in a rectangular slot

In this section we will develop a theoretical model of the response of a stratified fluid in a canyon to a horizontal pressure gradient imposed at the top of the canyon system. We want to demonstrate that water can be raised from a great depth to the continental shelf by this mechanism. The possibility can be demonstrated by a rough test of the energetics of the model, as follows. Water parcels from a (unknown) depth H must be raised to the depth of the continental shelf whereby their potential energy is increased. This is accomplished by the work done on the water parcels in the form of inward pressure gradient (force) times distance moved along the canyon. Using a simple model for the distribution of the geostrophic flow around the eddy, we compute the pressure gradient and find the depth H which balances potential energy change against work done. The result is that water can be drawn from up to 450 m depth and deposited on the shelf with zero kinetic energy. The scales involved suggest that speeds are around 1 cm/s; thus the kinetic energy density is very low, essentially zero within the limits of this calculation. In the standard upwelling problem most of the pressure-gradient force balances an alongshore geostrophic flow; and so energy sufficient to raise water parcels from great depth is not available.

We imagine the continental shelf to have a constant depth $H_o = -150$ m. The shelf is cut by a canyon of variable depth but constant width. At some position, $x = 0$, the canyon blends smoothly into the continental shelf, as we move seaward

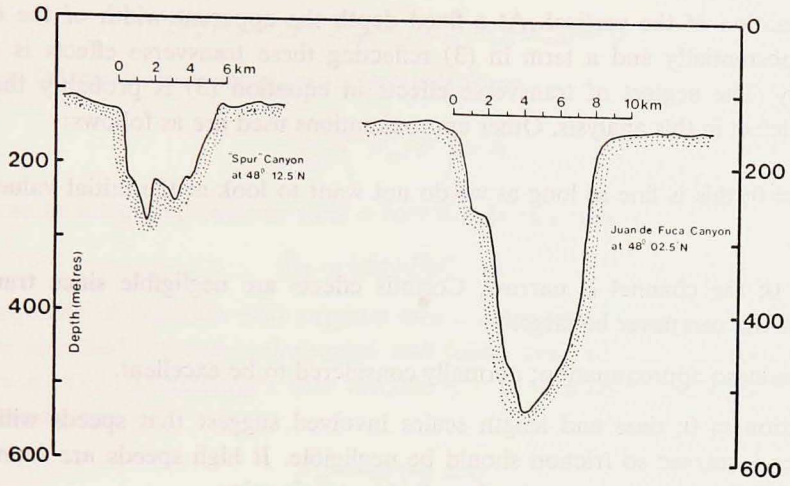

Figure 11. Sample depth sections across the local canyons.

along the canyon (x increasing) depth steadily increases and reaches a maximum at the shelf edge. The vertical coordinate will be taken as positive upward with $z = 0$ the free surface. The velocity components u and w are along-canyon and vertical components of velocity, respectively. All other variables take their usual interpretations. The equations of motion to be used are as follows:

$$\frac{\partial P}{\partial z} + \rho g = 0 \tag{1}$$

$$u\frac{\partial u}{\partial x} + w\frac{\partial u}{\partial z} = -\frac{1}{\rho_o}\frac{\partial P}{\partial x} \tag{2}$$

$$\frac{\partial u}{\partial x} + \frac{\partial w}{\partial z} = 0 \tag{3}$$

$$u\frac{\partial \rho}{\partial x} + w\frac{\partial \rho}{\partial z} = 0 \tag{4}$$

In equation (1) we have used the hydrostatic approximation, normally considered to be a good approximation. In equation (2) the balance of terms is requiring that the longitudinal pressure gradient acts only to accelerate fluid parcels. Equation (4) implies that water parcels are advected without changing their properties. This is absolutely necessary since without the advection of density, baroclinic pressure gradients could not be established to oppose the barotropic gradients, and there would be no essential difference between barocline and barotropic flows. Equation (3) is contentious, simple though it may seem. As long as we are really dealing with a vertical-walled canyon, transverse velocities will be small and (3) is accurate. However, Figure 11 shows two actual profiles across the canyon system. By oceanographic standards the sides are very steep, about 1 in 7, but that is not a good

approximation of the vertical. At a fixed depth the apparent width of the canyon varies substantially and a term in (3) reflecting these transverse effects is strictly necessary. The neglect of transverse effects in equation (3) is probably the most serious defect in this analysis. Other approximations used are as follows:

i) $\frac{\partial}{\partial t} = 0$; this is fine as long as we do not want to look at the initial value problem.

ii) $f = 0$; the channel is narrow, Coriolis effects are negligible since transverse velocities can never be large.

iii) Boussinesq approximation; normally considered to be excellent.

iv) Friction = 0; time and length scales involved suggest that speeds will be of order 1 cm/sec so friction should be negligible. If high speeds are found then this will be seen *a posteriori* to be a bad approximation.

Equation (3) permits the definition of a stream-function field ψ such that

$$u = -\frac{\partial \psi}{\partial z} \text{ and } w = \frac{\partial \psi}{\partial x}.$$

Equation (4) implies that the Jacobian $J(\psi,\rho) = 0$ so we can write $\rho = \rho(\psi)$ alone.

Eliminating ρ between (4) and (1) yields:

$$uP_{xz} + wP_{zz} = 0 \ . \tag{5}$$

After some manipulation P can be eliminated from (5) using (2) yielding the equation:

$$2\psi_z\psi_x\psi_{xz}\psi_{xzz} + \psi_x\psi_z{}^2\psi_{xxzz} - 2\psi_x{}^2\psi_z\psi_{xzzz} - \psi_{xx}\psi_z{}^2\psi_{xzz} - \psi_x{}^2\psi_{zz}\psi_{xzz} + \psi_x{}^3\psi_{zzzz} = 0 \ . \tag{6}$$

It is immediately seen that a simple solution to this rather awkward looking equation exists in the form $\psi(x,z) = G(x)z$ where G is any arbitrary function of x. It is quite easily shown that this corresponds to the trivial case ρ = constant, the barotropic case. We will have more to say about this as a limit of baroclinic solutions later.

To find baroclinic solutions let us try separable forms for ψ,

$$\text{i.e., } \psi(x,z) = G(x)\,F(z) \ . \tag{7}$$

Substituting (7) in (6) yields

$$GG_x{}^3\,[2F_z{}^2F_{zz} - 2FF_zF_{zzz} - FF_{zz}{}^2 + F^2F_{zzzz}] = 0 \ .$$

Let G be any arbitrary function of x with the proviso that nowhere in the range of x of interest can $GG_x{}^3 = 0$ then we find:

$$2F_z{}^2F_{zz} - 2FF_zF_{zzz} - FF_{zz}{}^2 + F^2F_{zzzz} = 0 \ . \tag{8}$$

Equation (8) can be rearranged into a tractable form,

$$\frac{d^2}{dz^2}\left(F_{zz}/F \right) = 0$$

which can be integrated twice to yield a very simple equation:

$$F_{zz} - (Az+B)F = 0 \ . \tag{9a}$$

The simplicity of equation (9a) suggests that a more direct derivation might exist, we have searched for such a derivation and found none to date. Setting $a = A^{1/3}$ and $b = B/A^{2/3}$ and defining a new variable $\eta = az + b$ the above equation is put in the standard form:

$$F_{\eta\eta} - \eta F(\eta) = 0 \ . \tag{9b}$$

The general solution to equation (9), and so of equation (8) is, (see Abramowitz and Stegun, 1964):

$$F(\eta) = \alpha Ai(\eta) + \beta Bi(\eta) \ .$$

The second Airy function $Bi(\eta)$ behaves poorly, and since quite acceptable models can be developed without it we set, rather arbitrarily, $\beta = 0$ and so write the baroclinic solutions to (6) as

$$\psi(x,z) = G(x)\, Ai(az+b) \ . \tag{10}$$

The condition for static stability everywhere, that density increases downward, can only be satisfied if $Ai(\eta)Ai'(\eta) \geqslant 0$. This immediately implies that we cannot use the region $\eta \geqslant 0$. There are many regions for negative η where this condition is satisfied, however, in this model we will choose only the region closest to the origin and require

$$-2.338 \ldots \leqslant \eta \leqslant -1.0188 \ldots$$

If the free surface, $z = 0$, is to be a streamline then $b = -2.338 \ldots$, and if the deepest streamline intersects the slope at $z = -600$ m then $0.0 \geqslant a \geqslant -2.199 \times 10^{-3}$. When a is close to zero Ai' tends to a constant value and $Ai(\eta) \propto \eta$ and we reduce the problem to the barotropic case, the case of $a = -2.199 \times 10^{-3}\text{m}^{-1}$ gives the largest stratification obtainable with a separable model.

Substituting equation (10) into (2) yields an expression for the pressure gradient force

$$\frac{\partial P}{\partial x} = -\tfrac{1}{2}\rho_0 a^2 \frac{\partial G^2}{\partial x}\left(Ai'^2 - \eta Ai^2\right) \ . \tag{11}$$

At a fixed depth, say the top of the canyon ($z = -150$ m) the term in parentheses is

a constant, α, and we find a simple expression for $G(x)$ in terms of a model distribution of the pressure gradient imposed on the top of the canyon. We postulate that the pressure gradient is supplied by the unbalancing of the geostrophic flow just above the top of the canyon. Thus, above the canyon:

$$\frac{\partial P}{\partial x} = \rho_0 f v(x)$$

where $v(x)$ is the geostrophic flow across the channel, and we apply a simple model for $v(x)$,

$$v(x) = v_0\{x/R_0\}\exp(-x/R_0)$$

and in the following we use $v_0 = 41$ cm/s and $R_0 = 17$ km giving a maximum value of $v(x) = 15$ cm/s at $x = R_0$. A constant of integration appears in the definition of $G(x)$ from equation (11) and we find, with the model of $v(x)$ used above that

$$G(x) = G_0\left(\left(1 + \frac{x}{R_0}\right)\exp\left(-\frac{x}{R_0}\right) - C\right)^{1/2}$$

where

$$G_0 = (2fv_0R_0/\alpha a^2)^{1/2}\,.$$

Nowhere in the analysis so far has there been any mention of the longitudinal bottom profile along the canyon. Since the bottom boundary condition required is one of no flow normal to the boundary we choose to proceed as follows. The canyon depth is chosen to be $z = -150$ m at $x = 0$ km and $z = -600$ m at $x = 55$ km (the mouth of the Juan de Fuca Canyon) the constant C in the definition of $G(x)$ is adjusted until a single streamline passes through both of these points and that streamline is henceforward considered to be "the bottom." There is, of course, no flow normal to a streamline so it is an appropriate lower boundary condition. This procedure may seem arbitrary but is a well-known method of simulating a variable bottom and has been used in the problem of airflow over mountains (see Queney *et al.* (1960) for example).

Figure 12 shows streamline patterns for the barotropic and maximum baroclinic cases, with the real along-canyon depth profile (and the cross canyon geostrophic flow imposed above) for comparison. In the latter case the density difference between the surface and $z = -600$ m is about 1.25 sigma-t units, the observed difference being about 2.9 units. We suspect that somehow implicit in the search for separable solutions to the equation (6) is the assumption that stratification is weak. Nevertheless, the stratification is quite substantial, and furthermore the proportionality of the variation in density to $Ai^2(z)$ quite effectively simulates a thermocline at a depth of around 250 m, a little deeper than is observed. Integrating along a streamline that originates at $x = 55$ km (the edge of the continental shelf) theory predicts that water parcels from a depth of 400 m can be raised to the height of the

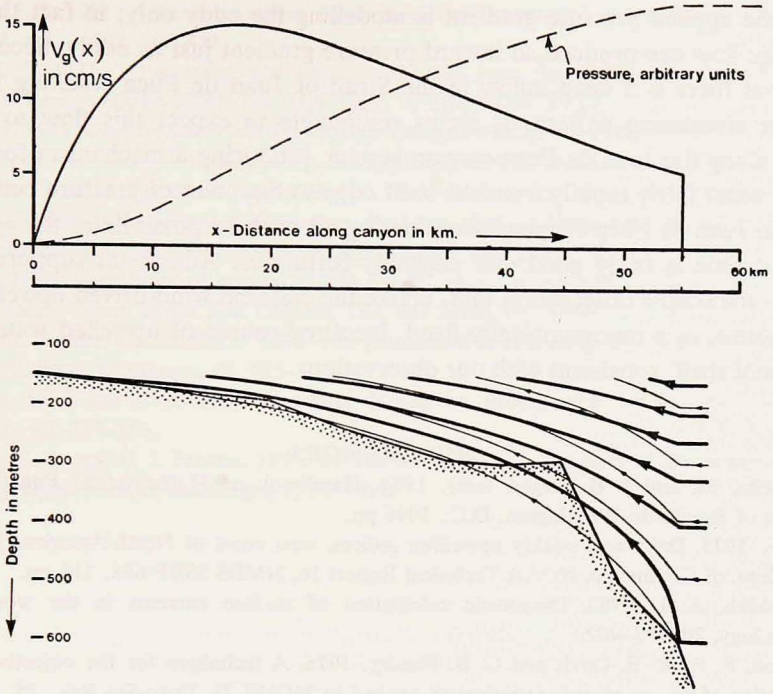

Figure 12. Streamlines of flow through the model canyon. Light lines are for the barotropic case and heavy lines for the baroclinic case. The observed depth profile along the talweg of the canyon system is superposed for comparison with the lowest streamline plotted in each case. Also shown above the contour plot are plots of the geostrophic speed, and associated pressure, distribution imposed at the top of the model canyon.

continental shelf in 30 days (for the barotropic case) and 93 days (for the large stratification case). If we presume that the inward pressure gradient is initiated at the time of the spring transition, and that water from the mouth of the Juan de Fuca Canyon is arriving on the shelf when we see the rapid decline in dissolved oxygen, Figure 2, then the transit time along the canyon was 78 days in 1980 and 97 days in 1981. Thus the observed transit time is predicted quite well by the baroclinic case.

Figure 12 also shows that the streamlines penetrate much deeper in the barotropic case compared with the baroclinic solution, and this is not surprising. However, it does pose a warning that if a highly baroclinic solution to equation (6) could be found (presumably a nonseparable solution) then the streamlines would penetrate even less. Since it is permitted, energetically, to raise water from a depth of 450 m to the shelf a highly baroclinic solution should demonstrate that, but the time taken to get onto the shelf must be expected to be greater. The time observed to transit the canyon system is observed to be around 80 days. There are two influences that might speed up the inflow even with a larger vertical stratification.

Firstly the applied pressure gradient is modelling the eddy only; in fact the steady shelf edge flow can produce an inward pressure gradient just as easily. Secondly, we know that there is a deep inflow in the Strait of Juan de Fuca resulting from the estuarine circulation pattern. It seems reasonable to expect this flow to be continuous along the Juan de Fuca canyon system, producing a mechanism for moving oceanic water fairly rapidly from the shelf edge to the point of juncture between the Spur and Juan de Fuca canyons. Considering all of these possibilities the agreement in transit time is fairly good and probably fortuitous. Additional support for this model is the simple observation that, unlike the classical wind-driven upwelling, this model results in a topographically-fixed, *localized* source of upwelled water on the continental shelf, consistent with our observations.

REFERENCES

Abramowitz, M. and I. E. Stegun (eds). 1964. Handbook of Mathematical Functions. Nat. Bureau of Standards, Washington, D.C., 1046 pp.

Bakun, A. 1975. Daily and weekly upwelling indices, west coast of North-America, 1967-1973. U.S. Dept. of Commerce, NOAA Technical Report 16, NMFS SSRF-693, 114 pp.

Brekhovskikh, A. L. 1980. Diagnostic calculation of surface currents in the world ocean. Oceanology, *20*, 398–402.

Bretherton, F. P., R. E. Davis and C. B. Fandry. 1976. A technique for the objective analysis and design of oceanographic experiments applied to MODE-73. Deep-Sea Res., *23*, 559–582.

Bryden, H. L. 1978. Mean upwelling velocities on the Oregon continental shelf during summer 1973. Estuar. Coast. Mar. Sci., *7*, 311–327.

Crawford, W. and R. E. Thomson. 1982. Continental shelf waves of diurnal period along Vancouver Island. J. Geophys. Res., (in press).

Denman, K. L., D. L. Mackas, H. J. Freeland, M. J. Austin and S. H. Hill. 1981. Persistent upwelling and meso-scale zones of high productivity off the west coast of Vancouver Island, Canada, *in* Coastal Upwelling, F. Richards, ed., American Geophysical Union, Washington, D.C., 514–521.

Halpern, D. 1976. Structure of a coastal upwelling event observed off Oregon during July 1973. Deep-Sea Res., *23*, 495–508.

Hickey, B. 1979. The California current system—hypotheses and facts. Progress in Oceanography, *8*, 191–279.

Huggett, W. S., J. F. Bath and A. Douglas. 1976. Data record of current observations, Volume XV, Juan de Fuca Strait 1973. Institute of Ocean Sciences, Sidney, B.C., Canada.

Huyer, A., R. L. Smith and E. J. C. Sobey. 1978. Seasonal differences in low-frequency fluctuations over the continental shelf. J. Geophys. Res., *83*, 5077–5089.

Huyer, A., E. J. C. Sobey and R. L. Smith. 1979. The spring transition in currents over the continental shelf. J. Geophys. Res., *84*, 6995–7011.

Kundu, P. K. and J. S. Allen. 1976. Some three-dimensional characteristics of low frequency current fluctuations near the Oregon coast. J. Phys. Oceanogr., *6*, 181–199.

Mackas, D. L., G. C. Louttit and M. J. Austin. 1980. Spatial distribution of zooplankton and phytoplankton in British Columbia coastal waters. Can. J. Fish. Aquat. Sci., *37*, 1476–1487.

Mackas, D. L. and H. A. Sefton. 1982. Plankton species assemblages off southern Vancouver Island: Geographic pattern and temporal variability. J. Mar. Res., *40*, 1173–1200.

McCreary, J. P. 1981. A linear stratified ocean model of the coastal undercurrent. Phil. Trans. R. Soc. Lond., *A302*, 385–413.

Nelson, C. S. 1977. Wind stress and wind stress curl over the California Current. NOAA Technical Report NMFS SSRF-714, U.S. Dept. of Commerce, 89 pp.

Pedlosky, J. 1979. Geophysical Fluid Dynamics. Springer-Verlag, New York, 624 pp.

Queney, P., G. A. Corby, N. Gerbier, H. Koschmieder and J. Zierep. 1960. The airflow over mountains. W.M.O. Technical Report No. 34, W.M.O., Geneva, Switzerland, 135 pp.

Stucchi, D. J. 1982. Shelf-fjord exchange on the west coast of Vancouver Island. Proceedings of a workshop on Coastal Oceanography, Bergen, Norway, June 1982.

Tabata, S. 1965. Variability of oceanographic conditions at Ocean Station "P" in the northeast Pacific Ocean. Trans. Royal Soc. Canada, Vol. III: Series IV: 367–418.

Thomson, R. E. and W. Crawford. 1982. The generation of diurnal period shelf waves by tidal currents. J. Phys. Oceanogr., *12*, 635–643.

Veronis, G. 1972. On properties of seawater defined by temperature, salinity and pressure. J. Mar. Res., *30*, 227–255.

Weatherly, G. L. and P. J. Martin. 1978. On the structure and dynamics of the oceanic bottom boundary layer. J. Phys. Oceanogr., *8*, 557–570.

Received: *23 April, 1982*; revised: *3 August, 1982.*